JOURNAL OF COMPUTATIONAL PHYSICS 36, 55–70 (1980)

A Nonreflecting Outflow Boundary Condition for Subsonic Navier–Stokes Calculations

DAVID H. RUDY

NASA Langley Research Center, Hampton, Virginia 23665

AND

JOHN C. STRIKWERDA*

Institute for Computer Applications in Science and Engineering (ICASE) Hampton, Virginia 23665

Received March 20, 1979; revised August 10, 1979

A nonreflecting boundary condition is presented for the numerical solution of the time-dependent compressible Navier–Stokes equations when these equations are used to obtain a steady state. This boundary condition is shown to be effective in reducing reflections at a subsonic outflow boundary. Numerical calculations using a model problem were made to compare this boundary condition with other outflow boundary conditions. The non-reflecting boundary condition contains a parameter whose optimal value is estimated using the analysis of a simplified set of equations.

I. INTRODUCTION

In the computation of solutions to the Navier-Stokes equations one of the chief difficulties is the numerical treatment of boundaries across which the fluid passes. This is especially true of subsonic outflow boundaries. In this paper several treatments of subsonic outflow boundaries are discussed and a new nonreflecting boundary condition is proposed. The emphasis is on obtaining the steady-state solution rather than the transient solution.

The Navier–Stokes equations require one boundary condition at a subsonic outflow boundary (see Oliger and Sundström [6]). One physical quantity that is readily measurable in many subsonic flow experiments is static pressure. Therefore in this paper it will be assumed that pressure is the only physical quantity that is known at the outflow boundary of the computational domain. In addition, in many cases the outflow boundary can be located so that the pressure is known to be a constant along that boundary.

* The research for the second author was supported under NASA Contract NAS1-14101 while he was in residence at ICASE, NASA Langley Research Center, Hampton, Va. 23665.

0021-9991/80/070055–16$02.00/0

The above considerations naturally lead one to impose the boundary condition that the pressure along the outflow boundary is held fixed at a known value i.e.,

$$p_{\text{out}} = p_\infty . \tag{1.1}$$

This boundary condition is well posed (see Oliger and Sundström [6]) and often works very well computationally; however, in certain problems, especially those in which one is seeking the steady-state solution of the Navier–Stokes equations, it can reflect pressure disturbances back into the computational domain. These disturbances can set up standing waves that are damped only very slowly by viscous and dissipative effects, and so inhibit convergence to steady state. This behavior is illustrated by the computations discussed in later sections.

Recently, there have appeared papers by Engquist and Majda [2] and Hedstrom [4] dealing with nonreflecting boundary conditions for partial differential equations. Nonreflecting boundary conditions are those that inhibit the reflection of disturbances incident on the boundary. The purpose of this paper is to examine these papers from a computational standpoint and to present a nonreflecting boundary condition for the compressible Navier–Stokes equations that can be applied at subsonic outflow boundaries. The various boundary conditions are compared using a model problem and suggestions are given for their use in more realistic computational problems. The results of this paper are stated for the viscous Navier–Stokes equations but clearly they are applicable to the inviscid (i.e., Euler) equations as well.

The reader is referred to the paper of Gustafsson and Kreiss [3] for a more general analysis of computational boundary conditions.

II. Nonreflecting Boundary Conditions

In this section the techniques of Engquist and Majda [2] and Hedstrom [4] are applied to the Navier–Stokes equations. Because the Navier–Stokes equations are nonlinear and not hyperbolic, due to the viscous terms, the results of Engquist and Majda cannot be applied directly. Therefore only the linearized, inviscid equations will be treated. Let $\bar{\rho}, \bar{u}, \bar{v}$, and $\bar{p}$ represent a steady-state solution to the inviscid Navier–Stokes equations and let $\tilde{\rho}, \tilde{u}, \tilde{v}$, and $\tilde{p}$ be perturbations about that state. The equations to first order in the perturbation variables are

$$\begin{pmatrix} \tilde{\rho} \\ \tilde{u} \\ \tilde{v} \\ \tilde{p} \end{pmatrix}_t + \begin{pmatrix} \bar{u} & \bar{\rho} & 0 & 0 \\ 0 & \bar{u} & 0 & \bar{\rho}^{-1} \\ 0 & 0 & \bar{u} & 0 \\ 0 & \gamma\bar{p} & 0 & \bar{u} \end{pmatrix} \begin{pmatrix} \tilde{\rho} \\ \tilde{u} \\ \tilde{v} \\ \tilde{p} \end{pmatrix}_x + \begin{pmatrix} \bar{v} & 0 & \bar{\rho} & 0 \\ 0 & \bar{v} & 0 & 0 \\ 0 & 0 & \bar{v} & \bar{\rho}^{-1} \\ 0 & 0 & \gamma\bar{p} & \bar{v} \end{pmatrix} \begin{pmatrix} \tilde{\rho} \\ \tilde{u} \\ \tilde{v} \\ \tilde{p} \end{pmatrix}_y = 0. \tag{2.1}$$

The region of interest is the half-plane $x \leqslant L$, $y \in \mathbb{R}$, $t \geqslant 0$, and assume that at $x = L$,

$$0 < \bar{u} < \bar{c} = (\gamma\bar{\rho}^{-1}\bar{p})^{1/2},$$

so that this is a subsonic outflow boundary.

The first approximation of Engquist and Majda [2] is

$$\tilde{p} - \bar{\rho}\bar{c}\tilde{u} = 0$$

or, equivalently,

$$p - \bar{\rho}\bar{c}u = \bar{p} - \bar{\rho}\bar{c}\bar{u}. \tag{2.2}$$

The quantity $\tilde{p} - \bar{\rho}\bar{c}\tilde{u}$ is the incoming characteristic variable for the one-dimensional problem obtained by neglecting the terms with y derivatives in Eq. (2.1).

The boundary condition (2.2) was tried in a model problem for which the steady-state values of all the variables were known (see Section IV) and it achieved the steady-state solution much faster than did boundary condition (1.1). However, in general the steady-state values of all the variables are not known a priori and therefore boundary condition (2.2) cannot be used in general. The second approximation of Engquist and Majda is of the form

$$\frac{\partial}{\partial t}(\tilde{p} - \bar{\rho}\bar{c}\tilde{u}) + c_1\tilde{\rho} + c_2\tilde{u} + c_3\tilde{v} + c_4\tilde{p} + c_5\frac{\partial\tilde{v}}{\partial y} = 0, \tag{2.3}$$

where the coefficients c_i involve $\bar{\rho}$, $\bar{u}$, $\bar{v}$, and $\bar{p}$ and their spatial derivatives. Again the difficulty is that all the steady-state values are not known.

Hedstrom [4] has recently obtained a nonreflecting boundary condition for the nonlinear one-dimensional inviscid Navier–Stokes equations. His boundary condition is equivalent to

$$\frac{\partial p}{\partial t} - \rho c\frac{\partial u}{\partial t} = 0. \tag{2.4}$$

Hedstrom shows that outgoing simple waves produce no reflections when boundary condition (2.4) is used.

Note that boundary condition (2.4) requires no a priori knowledge of the steady-state values of the variables. This has the result that the steady-state solution is dependent on the initial data; in particular, the steady-state pressure may not be $\bar{p}$. Since the emphasis in this paper is on the steady-state subsonic solution rather than the transient solution emphasized by Hedstrom, boundary condition (2.4) is not satisfactory.

In analogy with both boundary conditions (2.3) and (2.4), consider

$$\frac{\partial p}{\partial t} - \rho c\frac{\partial u}{\partial t} + \alpha(p - \bar{p}) = 0, \tag{2.5}$$

where α is some number to be determined. This boundary condition has the advantage that it gives precisely the right amount of boundary data because if a steady-state solution is achieved then the outflow pressure will be the desired value. However, it has the disadvantage of requiring the specification of the parameter α.

In the next section the optimum value for the parameter α is obtained for the case of linearized one-dimensional equations and in the last section computational results are presented for the Navier–Stokes equations in two dimensions. In Section V it is shown that a good approximation of the optimal parameter α can be given and that with a good choice of this parameter the steady-state solution can be obtained more readily.

Another way to treat the outflow boundary is to use a reference plane characteristic scheme such as Cline used [1] at the exit plane of a nozzle calculation. Three characterstic relations and the specified nozzle exit pressure form a system of four coupled equations for u, v, ρ, and p. Such a boundary condition is also nonreflecting; however, it requires many more operations and thus more computation time per time step than the present nonreflecting boundary condition.

Although the analysis in this paper is based on the inviscid equations, the computations with the model problem show that the results are applicable to the high-Reynolds-number viscous equations as well.

III. Determining α

In this section the optimal choice of the parameter α for boundary condition (2.5) is determined for a linearized constant coefficient one-dimensional system of equations corresponding to the equations of fluid flow.

Consider the system

$$\begin{aligned} \frac{\partial u}{\partial t} + \bar{u}\,\frac{\partial u}{\partial x} + \frac{1}{\bar{\rho}}\,\frac{\partial p}{\partial x} &= 0, \\ \frac{\partial p}{\partial t} + \bar{u}\,\frac{\partial p}{\partial x} + \gamma\bar{p}\,\frac{\partial u}{\partial x} &= 0, \end{aligned} \tag{3.1}$$

which is a linearized system for u and p, the deviations from the steady-state solution. The steady-state values $\bar{u}$, $\bar{p}$, and $\bar{\rho}$ are positive constants, and $0 \leqslant x \leqslant L$, $t \geqslant 0$. The boundary conditions are

$$u(0, t) = 0 \qquad \text{at} \quad x = 0,$$

$$\frac{\partial p}{\partial t} - \bar{\rho}\bar{c}\,\frac{\partial u}{\partial t} + \alpha p = 0 \qquad \text{at} \quad x = L.$$

The optimal choice for the parameter α is that value which makes the deviations u and p tend to zero most rapidly.

It is assumed that

$$0 < \bar{u} < \bar{c} = (\gamma\bar{\rho}^{-1}\bar{p})^{1/2}$$

so that the boundary at $x = L$ is a subsonic outflow boundary.

The solution to system (3.1) is a superposition of solutions of the form

$$\begin{aligned} u &= \quad e^{-z(t-\lambda x)} - e^{-z(t-\mu x)}, \\ p &= \bar{\rho}\bar{c}(e^{-z(t-\lambda x)} + e^{-z(t-\mu x)}), \end{aligned} \tag{3.2}$$

where $\lambda = (\bar{u} + \bar{c})^{-1}$ and $\mu = (\bar{u} - \bar{c})^{-1}$ and the values of z are to be determined by the boundary condition at $x = L$.

Substituting solutions (3.2) in the boundary condition at $x = L$ results in

$$0 = \bar{\rho}\bar{c}e^{-z(t-\mu x)} \cdot \{-2z + \alpha(1 + e^{z(\lambda-\mu)L})\} = 0.$$

Set

$$\tau = L(\lambda - \mu) = 2L\bar{c}/(\bar{c}^2 - \bar{u}^2) > 0;$$

then the equation relating α and z is

$$\alpha = 2z/(1 + e^{z\tau}). \tag{3.3}$$

This relation determines an infinite set of complex functions $z_m(\alpha)$ defined for all real values of α. The optimum α is that for which the real parts of all the $z_m(\alpha)$ are as large as possible. That is, choose α so that the transient solution to Eqs. (3.1) decays most rapidly. Note that when $\alpha < 0$, then Re $z < 0$, so only positive values of α need to be considered.

Set $\zeta = z\tau$ and $\sigma = 2/(\alpha\tau)$. Then Eq. (3.3) becomes

$$\sigma = (1 + e^{\zeta})/\zeta, \qquad 0 \leqslant \sigma < \infty. \tag{3.4}$$

This equation defines an infinite set of functions $\zeta_m(\sigma)$ where ζ_m is determined by

$$\zeta_m(0) = m\pi i, \qquad m = \pm 1, \pm 3, \pm 5, \ldots.$$

Note that ζ_m is defined only for odd m, and $\bar{\zeta}_m(\sigma) = \zeta_{-m}(\sigma)$ when $\zeta_m(\sigma)$ is not real. Two constants that are important in the following are ζ^* and σ^* defined by

$$\begin{aligned} \zeta^* &= 1 + e^{-\zeta^*} = 1.2784645, \\ \sigma^* &= e^{\zeta^*} \qquad = 3.5911214. \end{aligned}$$

ζ^* is that real value of ζ that gives the least value of σ in Eq. (3.4), and σ^* is that least value. The functions $\zeta_m(\sigma)$ for $m \neq \pm 1$ are well-defined functions for all nonnegative values of σ. However, $\zeta_1(\sigma)$ and $\zeta_{-1}(\sigma)$ are only well defined in the interval $0 \leqslant \sigma \leqslant \sigma^*$. At $\sigma = \sigma^*$,

$$\zeta_1(\sigma^*) = \zeta_{-1}(\sigma^*) = \zeta^*.$$

These functions can be extended for all nonnegative values σ by setting

$$\zeta_{-1}(\sigma) < \zeta^* < \zeta_1(\sigma) \qquad \text{for } \sigma > \sigma^*,$$

where $\zeta_1(\sigma)$ and $\zeta_{-1}(\sigma)$ are the two real branches determined by Eq. (3.4).

The next theorem gives the optimal choice of σ and α.

THEOREM. *The following relation holds:*

$$\max_{0<\sigma<\infty} \min_{m} \operatorname{Re} \zeta_m(\sigma) = \zeta^*;$$

therefore the optimal choice for α is

$$\alpha^* = \frac{\bar{c}^2 - \bar{u}^2}{\bar{c}L} (\zeta^* - 1). \tag{3.5}$$

Proof. The proof is in two parts. The first part considers $\zeta_m(\sigma)$ only for $|m| > 1$. It is shown for these values of m that $\operatorname{Re} \zeta_m(\sigma) > \zeta^*$ for $\sigma > \sigma^*$. This requires showing that $\operatorname{Re} \zeta_m(\sigma)$ is unbounded as σ increases. Next it is shown that $\operatorname{Re} \zeta_{-1}(\sigma) \leqslant \zeta^*$ for all σ. Since $\zeta_{-1}(\sigma^*) = \zeta^*$ this will complete the proof.

From Eq. (3.4) it follows that

$$\sigma \operatorname{Im} \zeta_m(\sigma) = \operatorname{Im} e^{\zeta_m(\sigma)}.$$

Since the right side of the above vanishes when $\operatorname{Im} \zeta_m(\sigma)$ is an integer multiple of π, for $0 < \sigma < \infty$ the imaginary part of $\zeta_m(\sigma)$ cannot be a nonzero integer multiple of π.

Since $\zeta_m(0) = m\pi i$, this shows that

$$|\operatorname{Im} \zeta_m(\sigma) - m\pi| < \pi, \qquad |m| \neq 1.$$

Consider now only m with $|m| \neq 1$. From the above

$$\sigma(|m| - 1)\pi < \sigma |\operatorname{Im} \zeta_m(\sigma)| < e^{\operatorname{Re} \zeta_m}.$$

This shows that $\operatorname{Re} \zeta_m(\sigma)$ is unbounded as σ increases. Therefore $\operatorname{Re} \zeta_m(\sigma) = \zeta^*$ for some value of σ.

From Eq. (3.4) it follows that

$$\sigma \operatorname{Re} \zeta_m < 1 + e^{\operatorname{Re} \zeta_m}.$$

Because the inequality

$$\sigma^* \leqslant (1 + e^x)/x$$

holds for all real x, with equality only for $x = \zeta^*$, it follows that when $\operatorname{Re} \zeta_m = \zeta^*$ then $\sigma < \sigma^*$. Since $\operatorname{Re} \zeta_m > \zeta^*$ for large σ it must hold that $\operatorname{Re} \zeta_m > \zeta^*$ for all $\sigma \geqslant \sigma^*$.

Consider now $m = \pm 1$. First it will be shown that for $0 \leqslant \sigma < \sigma^*$,

$$\operatorname{Re} \zeta_1(\sigma) = \operatorname{Re} \zeta_{-1}(\sigma) \leqslant \zeta^*$$

with equality only for $\sigma = \sigma^*$.

From Eq. (2.4) and $\sigma^* = e^{\zeta^*}$ one obtains

$$\begin{aligned}\sigma\zeta - \sigma^*\zeta^* &= e^{\zeta} - e^{\zeta^*} \\ &= \sigma^*(e^{\zeta-\zeta^*} - 1).\end{aligned}$$

If $\zeta = \zeta^* + i\theta$, then

$$(\sigma - \sigma^*)\,\zeta^* = \sigma^*(\cos\theta - 1),$$

and

$$\sigma\theta = \sigma^* \sin\theta.$$

Eliminating σ from the above two equations yields the equations

$$\zeta^*(1 - \sin\theta/\theta) = 1 - \cos\theta.$$

But for $|\theta| < \pi$

$$2(1 - \sin\theta/\theta) \leqslant 1 - \cos\theta,$$

and since $\zeta^* < 2$, it follows that Re $\zeta_1(\sigma) = \zeta^*$ only for $\theta = 0$, and

$$\text{Re}\,\zeta_1(\sigma) < \zeta^* \qquad \text{for } 0 < \sigma < \sigma^*.$$

Moreover, for $\sigma > \sigma^*$ the value of $\zeta_{-1}(\sigma)$ is less than ζ^*. This proves the first relation in the theorem.

Relating the above results to the parameter α, one sees that for maximum damping of the transient solution of Eq. (3.1), α should be chosen so that

$$\alpha = \alpha^* = \frac{2}{\sigma^*\tau} = \frac{\bar{c}^2 - \bar{u}^2}{\bar{c}L}(\zeta^* - 1).$$

This proves the theorem.

For σ near σ^*, $\zeta_{\pm1}(\sigma)$ have the expansions

$$\begin{aligned}\zeta_{\pm1}(\sigma) = \zeta^* &\pm [2\zeta^*(\zeta^* - 1)]^{1/2}(\sigma - \sigma^*)^{1/2} \\ &+ \tfrac{1}{3}(\zeta^* - 1)(3 - \zeta^*)(\sigma - \sigma^*) + O(\sigma - \sigma^*)^{3/2}\end{aligned}$$

and hence for $\sigma < \sigma^*$

$$\text{Re}\,\zeta_{\pm1}(\sigma) \cong \zeta^* - 0.16(\sigma^* - \sigma) + O(\sigma - \sigma^*)^2$$

and for $\sigma > \sigma^*$

$$\text{Re}\,\zeta_{-1}(\sigma) \cong \zeta^* - 0.84(\sigma - \sigma^*)^{1/2} + O(\sigma - \sigma^*).$$

From this it is apparent that in estimating α it is better to overestimate α (i.e., use a smaller value of σ) rather than to underestimate α.

IV. Test Problems

Solutions were obtained to the time-dependent two-dimensional compressible Navier–Stokes equations for two model problems to compare the present non-reflecting boundary condition (2.5) with two other boundary conditions.

The equations describing the conservation of mass, momentum, and energy may be written in dimensionless conservation form as

$$\frac{\partial U}{\partial t} + \frac{\partial F}{\partial x} + \frac{\partial G}{\partial y} = 0, \tag{4.1}$$

where

$$U = \begin{bmatrix} \rho \\ \rho u \\ \rho v \\ E \end{bmatrix},$$

$$F = \begin{bmatrix} \rho u \\ \rho u^2 + p - \tau_{xx} \\ \rho uv - \tau_{xy} \\ (E + p - \tau_{xx})u - \tau_{yx}v - \dfrac{\gamma k}{\sigma R}\dfrac{\partial T}{\partial x} \end{bmatrix},$$

$$G = \begin{bmatrix} \rho v \\ \rho uv - \tau_{yx} \\ \rho v^2 + p - \tau_{yy} \\ (E + p - \tau_{yy})v - \tau_{xy}u - \dfrac{\gamma k}{\sigma R}\dfrac{\partial T}{\partial y} \end{bmatrix},$$

and where

$$\tau_{xx} = \frac{\mu}{R}\left(\frac{4}{3}\frac{\partial u}{\partial x} - \frac{2}{3}\frac{\partial v}{\partial y}\right),$$

$$\tau_{xy} = \tau_{yx} = \frac{\mu}{R}\left(\frac{\partial u}{\partial y} + \frac{\partial v}{\partial x}\right),$$

$$\tau_{yy} = \frac{\mu}{R}\left(\frac{4}{3}\frac{\partial v}{\partial y} - \frac{2}{3}\frac{\partial u}{\partial x}\right),$$

in terms of density ρ, the x and y velocity components u and v, viscosity coefficient μ, specific total energy E, coefficient of heat conductivity k, and temperature T. σ and R are the dimensionless Prandtl number and Reynolds number, respectively, and γ is the ratio of specific heats. σ was taken to be 0.72 and γ was 1.4.

The flow was taken to be laminar and thus the viscosity is given by the Sutherland law. Finally, the pressure is related to the temperature and density by the equation of state

$$p = (\gamma - 1)\,\rho T. \tag{4.2}$$

These equations were advanced in time to a steady state using the unsplit MacCormack finite-difference algorithm [5] on the CDC STAR-100 computer. A forward-predictor, backward-corrector operator sequence was used for all time steps.

The model problems were chosen so that the effect of the outflow boundary conditions could be isolated without the complicating effects of geometry. The first problem is shown schematically in Fig. 1. The flow is a uniform subsonic flow in the x-direction with an interior two-dimensional perturbation at $t = 0$. The boundary conditions at inflow and at the upper and lower boundaries shown in Fig. 1 were used with several outflow boundary conditions. At a subsonic inflow boundary three of the variables must be specified for the problem to be well posed (see Oliger and Sundström [6]). A square 21×21 uniform grid was used in all cases with a 7×7 initial disturbance centered in the computational domain. Three cases were run with different values of the free-stream Mach number M_∞. The total temperature was taken to be initially constant throughout the field; however, the static temperature and pressure in the initial disturbance were twice the free-stream values. The Mach numbers for the free stream flow M_∞ and the disturbance M_i, as well as the Reynolds number R, were as follows:

M_∞	M_i	R
0.8	0.283	3488
0.6	0.212	2932
0.4	0.141	2129

The initial density field was then computed from the equation of state (Eq. (4.2)) using the local values of p and T.

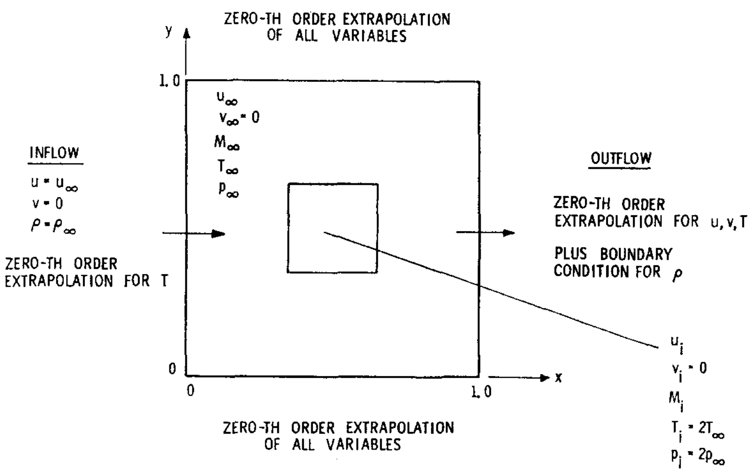

FIG. 1. Solution domain, initial conditions, and boundary conditions for the first test problem. The free-stream flow is given by the subscript ∞ and the initial disturbance is given by the subscript i.

The second problem is shown schematically in Fig. 2. A 41 $\times$ 21 grid was used, the solution domain was extended to $x = 2.0$, and the disturbance was centered at $x = 1.5$. The flow parameters and the size of the disturbance were the same as in the first problem.

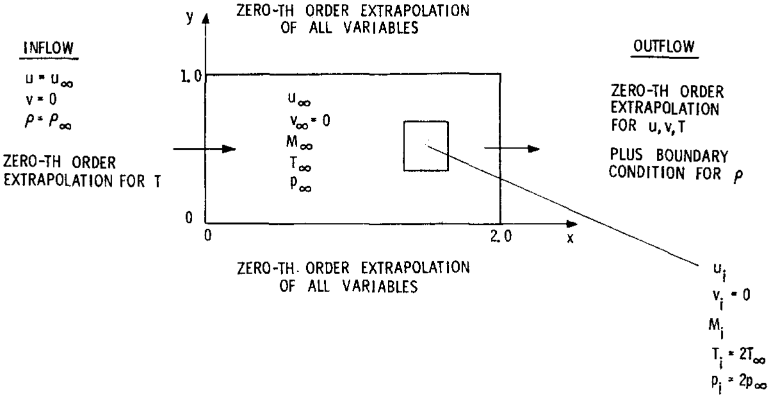

FIG. 2. Solution domain, initial conditions, and boundary conditions for the second test problem.

The three boundary conditions for density are given by the following, where the two subscripts refer to the x and y grid point indices, respectively, the superscripts refer to the time step, and NI is the last grid index in the x-direction.

(i) The present nonreflecting boundary condition:

$$\rho_{NI,j}^{n+1} = p_{NI,j}^{n+1}/(\gamma - 1)\, T_{NI,j}^{n+1}, \tag{4.3}$$

where $p_{NI,j}$ is computed from the finite-difference approximation to Eq. (2.5), i.e.,

$$p_{NI,j}^{n+1} = [p_{NI,j}^{n} + \alpha\, \Delta t\, p_\infty + \rho_{NI,j}^{n} c_{NI,j}^{n} (u_{NI,j}^{n+1} - u_{NI,j}^{n})] \frac{1}{1 + \alpha\, \Delta t}, \tag{4.4}$$

where $T_{NI,j}^{n+1}$ in (4.3) and $u_{NI,j}^{n+1}$ in (4.4) are the extrapolated values.

(ii) The constant-pressure boundary conditions:

$$\rho_{NI,j}^{n+1} \text{ is computed from (4.3) with } p_{NI,j}^{n+1} = p_\infty .$$

(iii) Extrapolation of density:

$$\rho_{NI,j}^{n+1} = \rho_{NI-1,j}^{n+1} . \tag{4.5}$$

In all three cases the outflow boundary condition was applied only after the corrector step. At the end of each predictor step the outflow boundary values were held at the previous corrected values. Note that boundary condition (ii) is the limit of boundary condition (i) as α tends to infinity.

Convergence to steady state was defined as occurring when the following condition was satisfied at every point in the field,

$$| \phi_{i,j}^{n+1} - \phi_{i,j}^{n} | \leqslant \epsilon, \tag{4.6}$$

where the subscripts i and j are the x and y grid point indices, respectively, the superscripts refer to the time step, and ϕ represents each dependent variable (u, v, ρ, T). $\epsilon = 10^{-8}$ was used for all calculations.

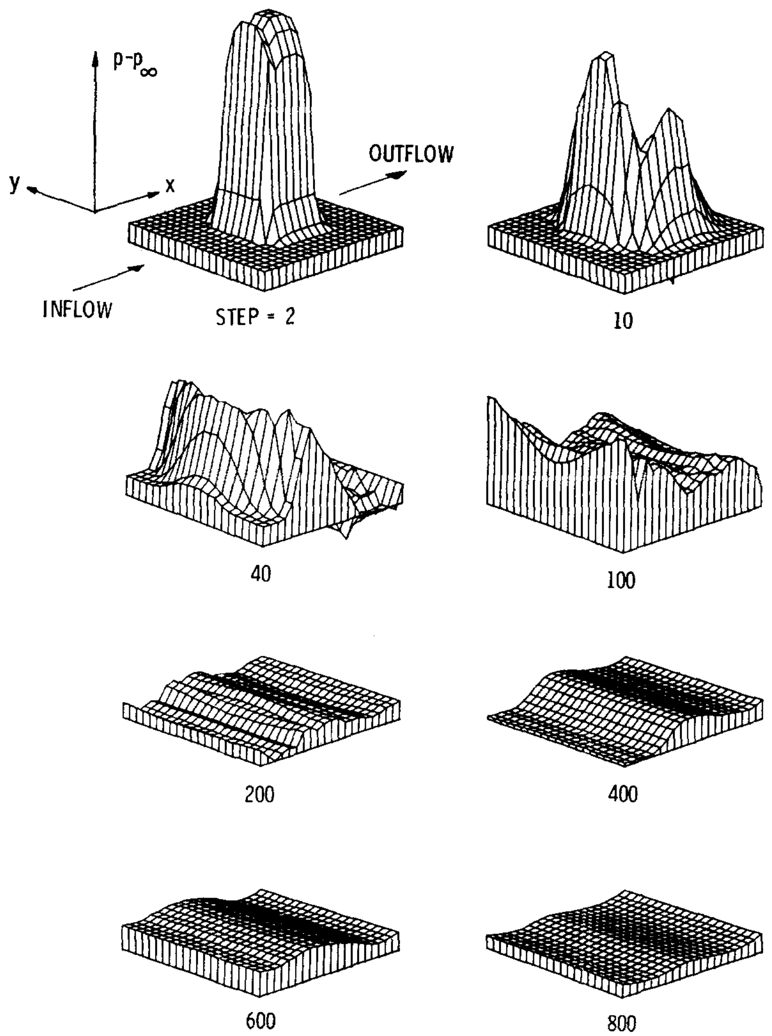

FIG. 3. Static pressure difference ($p - p_\infty$) for selected time steps using constant pressure outflow boundary condition.

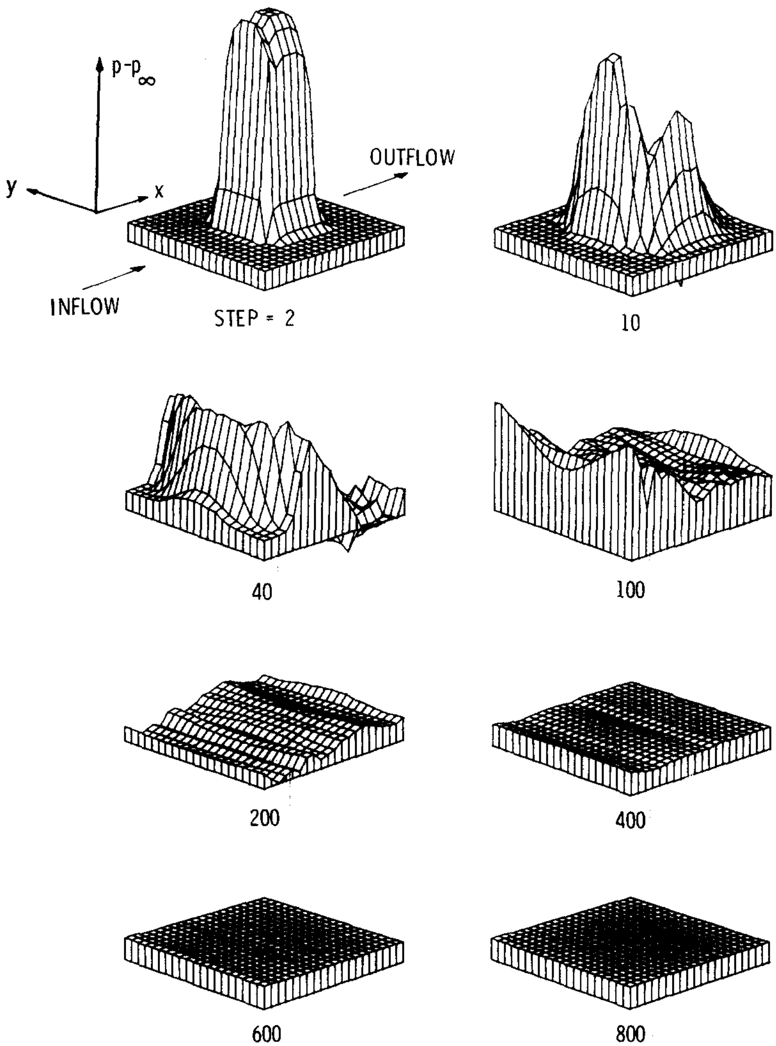

FIG. 4. Static pressure difference ($p - p_\infty$) for selected time steps using new nonreflecting outflow boundary condition. ($\alpha = 0.25$)

V. RESULTS

Figures 3 and 4 illustrate the advantage of the nonreflecting boundary condition (i) over the constant-pressure boundary condition (ii) for the first model problem with $M_\infty = 0.8$.

In Fig. 3 plots of the difference between calculated pressure and steady-state pressure ($p - p_\infty$) are presented for eight selected time steps for the constant-pressure boundary condition (ii). The first plot shows the disturbance after two time steps.

After 10 steps the initial wave has reached the outflow boundary and reflections have begun to occur. As the calculation proceeds waves continue to move back and forth across the computational domain with the amplitude of the waves continually decreasing. The calculation was continued for 20,000 steps, but did not converge for $\epsilon = 10^{-8}$; however, the maximum deviations in u, ρ, p, and v from their steady-state values were all less than 0.2 %.

Figure 4 shows plots of $p - p_\infty$ for the computation with the present nonreflecting boundary condition (i) with $\alpha = 0.25$ for the same eight times as in Fig. 3. The pressure fields for 2, 10, and 40 steps are very similar to those for the corresponding constant-pressure boundary condition case except near the outflow boundary. Boundary condition (i) adjusts the pressure at the outflow boundary so that the the disturbance is not fully reflected back into the computational domain. From the plots of steps 100 to 800 it can be seen that the pressure field with boundary condition (i) is settling to steady state much more rapidly than for the constant-pressure case. The solution for $\alpha = 0.25$ converged to a steady state ($\epsilon = 10^{-8}$) in 3383 steps.

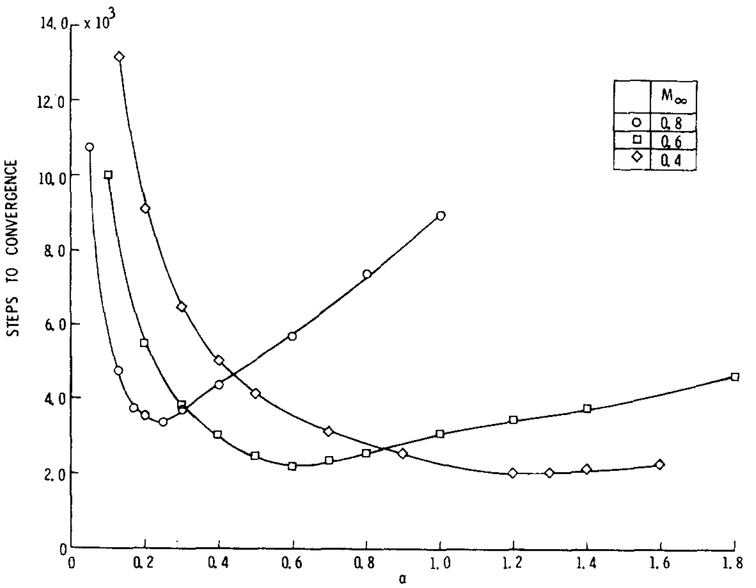

FIG. 5. Effect of α on convergence for the first test problem.

Boundary condition (i) was used with several values of the parameter α to study its effect on the convergence to steady state. Figures 5 and 6 show the number of time steps necessary to achieve convergence as a function of α for the different values of M_∞ in the first and second problems, respectively. An estimate of the optimal α can be made using Eq. (3.5) to compute α^*. The optimal α as determined from numerical experiments and α^* for the two problems are as follows

	Problem 1		Problem 2	
M_∞	α opt	α^*	α opt	α^*
0.8	0.25	0.13	0.125	0.06
0.6	0.60	0.31	0.30	0.15
0.4	1.2	0.59	0.65	0.29

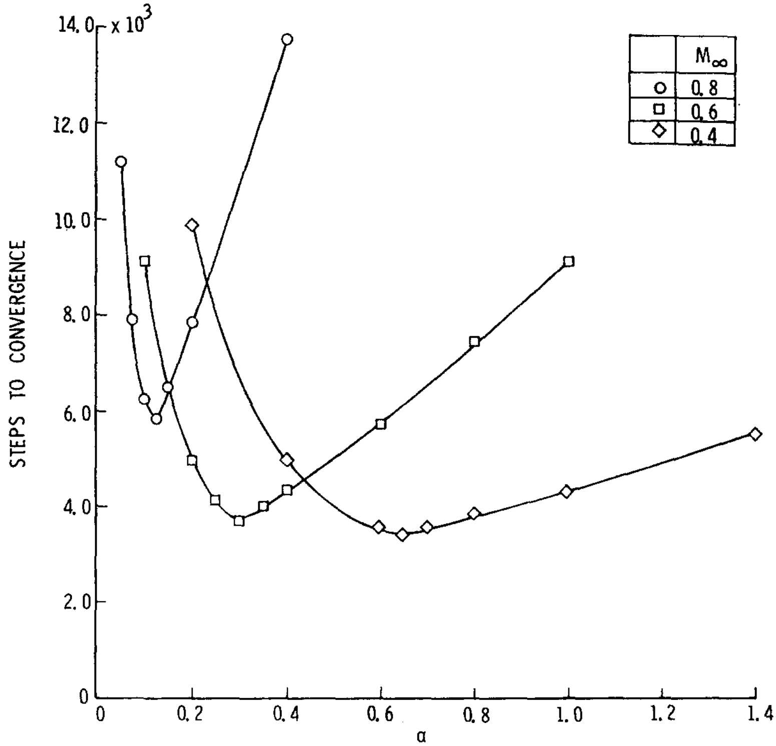

FIG. 6. Effect of α on convergence for the second test problem.

Note from Fig. 5 that for α equal to α^* the number of time steps needed to achieve convergence can be as much as twice that needed for the optimal α, but it is a significant improvement over boundary condition (ii), which did not reach convergence by 20,000 time steps. Of course since Eq. (3.5) was derived from the simplified system (3.1), one cannot expect strict agreement with the results for the two-dimensional nonlinear Navier–Stokes equations. It is apparent, therefore, that to estimate the optimal α for the Navier–Stokes equations one can use α^* from Eq. (3.5). Moreover, one might choose a somewhat larger value than α^* since, by the remarks at the end of Section III, an overestimation of the optimal α is expected to be less harmful than an underestimation of the same magnitude.

Figure 7 displays the number of time steps needed to achieve convergence to steady state as a function of the nondimensional quantity σ^{-1} as used in Section III, i.e.,

$$\sigma^{-1} = \frac{\alpha L}{(M_\infty^{-1} - M_\infty)\bar{u}} .$$

The striking similarity of the curves in Fig. 7 and their shape shows that the analysis of Section III is qualitatively correct. That is, the time needed to achieve steady state is determined largely by σ^{-1} independently of M_∞ and the length of the domain L.

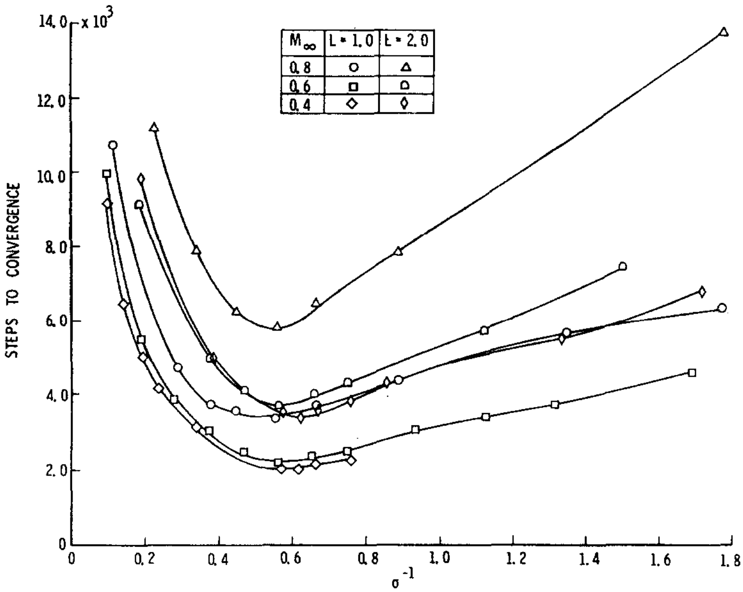

FIG. 7. Effect of σ^{-1} on convergence for both test problems.

Computations were also made using the first problem with $M_\infty = 0.8$ and both the boundary condition (iii), i.e., extrapolation of all variables, and boundary condition (i) with $\alpha = 0$. Boundary condition (iii) is not correct mathematically since the analysis indicates that one dependent variable should be specified and here all four are extrapolated. However, this boundary condition may be the only available option for some problems if no values of the dependent variables are known at the boundary. With extrapolation, the solution converged in only 2031 time steps, but to slightly incorrect values of temperature and hence pressure. With the $\alpha = 0$ boundary condition, convergence was reached in 1924 time steps and also to a slightly incorrect value of the temperature. Note that temperature is the one dependent variable which was extrapolated at the inflow boundary. In the present case the error in temperature changed the Mach number to 0.802 for boundary condition (iii) and to 0.793 for the $\alpha = 0$ boundary condition. These two boundary conditions were also used for a case in which the area of the initial distribution was much larger and extended to the outflow boundary. For the extrapolation boundary condition the Mach number was low by 21 % and for $\alpha = 0$ it was low by 33 %. This shows that with these boundary conditions the steady-state solution is strongly dependent on the initial flow field, which is a direct consequence of not specifying the steady-state pressure at the outflow boundary.

Conclusions

The nonreflecting boundary condition presented in this paper has been shown to be effective in reducing reflections at the subsonic outflow boundary for the compressible Navier–Stokes equations. It has been shown to be better than extrapolation and specification of the outflow pressure for the model problems considered.

These model problems did not have the complicating effects of solid-wall boundaries, separated flows, etc. However, the problems did have an initial disturbance large enough to produce substantial reflections at the outflow boundary. The conclusions might be altered in the presence of these complicating effects.

The time required for the model problems to attain steady state has been studied as a function of the parameter in the boundary condition. Moreover, its qualitative behavior has been shown to have the character predicted by the analysis of a simplified problem. This analysis also supplies a rough estimate of the optimal value of the parameter.

Acknowledgment

The authors acknowledge Dr. Eli Turkel for his helpful comments.

References

1. M. C. Cline, Report LA-5984, Los Alamos Scientific Laboratory, January 1977.
2. E. Engquist and A. Majda, *Math. Comput.* **31** (1977), 629–651.
3. B. Gustafsson and H. O. Kreiss, *J. Comput. Phys.* **30** (1979), 333–351.
4. G. W. Hedstrom, *J. Comput. Phys.* **30** (1979), 222–237.
5. R. W. MacCormack, "The Effect of Viscosity in Hypervelocity Impact Cratering," AIAA Hypervelocity Impact Conference, April 1969, AIAA Paper No. 69-354.
6. J. Oliger and A. Sundström, *SIAM J. Appl. Math.* **35** (1978), 419–446.